

M. Valovic, L. Garzotti, I. Voitsekhovitch, M. Beurskens, X. Garbet,
C Giroud, D Keeling and JET EFDA contributors

On the Correlation Between Density Profile and Particle Flux in H-Mode Tokamak Plasmas and the Implication for ITER

“This document is intended for publication in the open literature. It is made available on the understanding that it may not be further circulated and extracts or references may not be published prior to publication of the original when applicable, or without the consent of the Publications Officer, EFDA, Culham Science Centre, Abingdon, Oxon, OX14 3DB, UK.”

“Enquiries about Copyright and reproduction should be addressed to the Publications Officer, EFDA, Culham Science Centre, Abingdon, Oxon, OX14 3DB, UK.”

On the Correlation Between Density Profile and Particle Flux in H-Mode Tokamak Plasmas and the Implication for ITER

M. Valovic¹, L. Garzotti¹, I. Voitsekhovitch¹, M. Beurskens¹, X. Garbet²,
C Giroud¹, D Keeling¹ and JET EFDA contributors*

¹*EURATOM/UKAEA Fusion Association, Culham Science Centre, OX14 3DB, UK.*

²*Association EURATOM -CEA, CEA-Cadarache, 13108 Saint Paul Lez Durance France*

** See annex of J. Pamela et al, "Overview of JET Results",*

(Proc.20th IAEA Fusion Energy Conference, Vilamoura, Portugal (2004)).

ABSTRACT

Density peaking in tokamak ELMy H-mode plasmas is studied using data from the Joint European Torus (JET). It is shown that the electron density gradient and electron particle flux at mid radius are correlated when these two quantities are normalised to their heat-power-balance counterparts. Therefore the density profiles cannot be considered canonical and particle sources should be taken into account when extrapolating the density profiles to the ITER next step device. The relation between density and temperature gradients at mid radius is predicted in the range of $(\nabla n_e/n_e)/(\nabla T_e/T_e) \approx 0.15-0.35$ for plasmas with safety factor and collisionality similar to ITER standard discharge.

INTRODUCTION

Density peaking is one of the desired properties of tokamak plasmas as it produces higher fusion gain, providing it is not counter-balanced by unwanted accumulation of helium and other impurities in the core. Early limiter L-mode plasmas in tokamaks had peaked density profiles. With the introduction of magnetic divertors and H-mode operation, density pedestals appeared and profiles become flatter. The plasmas in future fusion reactors such as ITER are assumed to have flat density profiles [1]. Flattening of the density profiles in future devices could be even more pronounced because in larger and hotter plasmas the particle source due to gas puffing will be localised in the scrape-off layer and thus will not directly contribute to core fuelling. As a result, fuelling in reactors has to be arranged by injection of frozen fuel pellets. However, even with pellet fuelling the particle source is predicted to be localised in outer part of the plasma and thus cannot contribute to peaking of the density profile in the plasma core. Therefore the only possibility to realise a peaked density profile in burning plasmas seems to be the existence of a so-called anomalous (turbulence-driven) particle pinch.

For stationary plasmas, the particle pinch manifests itself as an existence of peaked density profiles under conditions when the particle source in the core is negligible. In H-mode plasmas, peaked density profiles have been reported in DIII-D [2, 3], Asdex-Upgrade [4] and JET [5]. These plasmas, however, had high densities and the particle pinch driven by the inductive electric field (Ware pinch) was significant, so that these results can not be extrapolated to next-step devices. Therefore more recent studies have concentrated on conditions where the role of the Ware pinch is small. With fully non-inductively-driven plasma current in Tore-Supra [6], and at low collisionalities in Asdex-Upgrade [7] and JET [8], [9], [10], the density profiles have been found to be peaked. Existence of an anomalous particle pinch also has support in equipartition theory [11] and is a consequence of the Fokker-Planck diffusion equation written for inhomogeneous plasmas [12]. In addition, peaked density profiles at zero particle flux have been predicted by fully nonlinear fluid simulations in the collisionless approximation [13].

One of the difficulties in extrapolation of density profiles from present plasmas towards reactor conditions is the role of particle sources. In a reactor such as ITER the core particle source is expected to be small, while in most of today's plasmas the particle source in the core can be significant. However, the role of the particle sources in today's plasmas has been a matter of debate. The importance of

particle sources from neutral-beam heating and wall neutrals in shaping the density profiles in JET H-mode plasmas has been highlighted in our previous publications [9, 14]. These studies show that even by replacing a significant fraction of the Neutral-Beam heating (NBI) by Radio-Frequency (RF) heating, the electron particle flux due to beams and wall neutrals at mid-radius is still not negligible and therefore extrapolation of the electron density gradient towards an ITER-like situation depends on the value of particle diffusivity. On the other hand the papers [8] and [15] are questioning the role of particle sources in shaping the density profile in today's tokamaks. In recent publications, however, the importance of particle source is recognised [16], [17]. Finally note that the question how strong is the dependence of density profiles on particle flux is related to the concept of canonical profiles as introduced for example in [11]. According to this theory the electron density in strongly turbulent plasmas has a tendency to arrange itself towards the canonical profile which depends only on the profile of safety factor.

This letter extends our previous studies [9] by addressing the uncertainty in the value of particle diffusivity and the correlation of particle flux with density gradient. Our focus is on prediction of density profiles in the ITER standard inductive plasma [1] and therefore we apply selection criteria to the JET data so that our dataset is as close as possible to such a condition. We include only: (i) ELMy H-mode plasmas with a conventional (monotonic) safety factor profile and without internal transport barrier, (ii) plasmas with a ratio of electron to ion temperatures close to $T_e/T_i \sim 1$, (iii) plasmas without neutral-beam counter (opposite of plasma current) injection, with one exception added for illustration and (iv) plasmas with values of safety factor and collisionality in the range of $q_{95} = 3.1-3.5$, $\nu_*/\nu_{*,ITER} = 1.3-3.3$. Here, collisionality normalised to the ITER value is defined as $\nu_*/\nu_{*,ITER} = (q_{95}/3) (R/6.2m)^{2.5} (a/2m)^{-1.5} (n_e/10^{20} \text{ m}^{-3}) (T_e/12keV)^{-2} (Z_{eff}/1.66)$, where R and a are the JET major and minor radii respectively; while electron density, n_e , electron temperature, T_e , and effective charge from charge-exchange spectroscopy, Z_{eff} , are evaluated at $a/R = 0.5$. Plasmas heated by NBI and RF or a combination of both are included in the dataset. It has to be noted that RF-heated plasmas have mainly type III ELMs while NBI-heated plasmas display type I ELMs. JET pulses used in the present study are mainly a subset of databases presented in papers [8], [9], [16] and are listed in the caption of figure 1.

The reason for restricting ourselves to plasmas with a narrow range of safety factor q_{95} and normalised collisionality ν_* is to eliminate possible correlation of particle flux with parameters other than density gradient. The safety factor or magnetic shear was reported to have a large impact on the density profile in L-mode plasmas [18, 19], though paradoxically this is not reported in H-modes [8, 16]. Concerning collisionality, this parameter is considered to be dominant in shaping the density profiles in H-mode plasmas [7, 8, 16]. Selection of the width of the intervals in q_{95} and ν_* is obviously a compromise between the desire to have these intervals as narrow as possible, but also to include enough data points to cover the whole range of particle flux and density gradients. It has to be said that those data with largest leverage for prediction of the density profile in ITER standard plasmas, i. e. with $q_{95} \approx 3.0$, $\nu_* \approx \nu_{*,ITER}$ and additionally heated only by RF, are very rare.

Two parameters are extracted from our dataset: electron particle-flux density normalised to heat-flux density, $\Gamma_e T_e / Q$, and electron density-gradient length normalised to electron temperature-gradient length, $(\nabla n_e / n_e) / (\nabla T_e / T_e)$. Here Q is the total heat-flux density including all plasma species. These quantities are evaluated in the stationary part of the plasma discharge to eliminate the contribution of $\partial t / \partial n_e$ to T_e , and taking only one data point per pulse. Spatially both quantities are taken at half of the plasma minor radius. The electron particle flux Γ_e (due to neutral beams and wall neutrals) and the heat flux Q (due to NBI, RF, OH heatings) are calculated with the TRANSP code [20, 21]. The fluxes are calculated by integrating the particle and heat sources and losses over the volume inside the given flux surface. Particle deposition profiles due to neutral beams are calculated in TRANSP by Monte-Carlo module NUBEAM. Particle source from wall neutrals are determined in TRANSP by FRANTIC module where the boundary condition use the experimental gas valve rate and the D_α photon flux. Detail discussion of boundary condition for FRANTIC module and sensitivity study can be found in our previous work [9]. Careful transport analysis for each data point was found to be essential because the ratio of particle to heat flux Γ_e / Q is not constant across the minor radius and therefore its value at half radius cannot be approximated by its edge value using the total neutral-beam power and the total heating power. This is particularly important for plasmas with a substantial fraction of RF heating power or pure RF heating, where the particle deposition profile and total heating profiles differ significantly. The density and temperature gradients are calculated from LIDAR data using the outboard side of the profiles. To enhance signal to noise, the LIDAR data are averaged over a 1 s time window. The gradients are calculated by linear regression over the range of normalised poloidal flux coordinates $0.35 \leq \sqrt{\psi_N} \leq 0.8$; this procedure is similar to that used in [9]. Such a restriction to the so called gradient zone should eliminate effects of sawteeth and ELMs on particle transport, so that the dataset reflects mainly properties of the turbulent particle flux. It has to be noted that even such a narrowing of the spatial domain cannot exclude possible local flattening of the density profile by tearing modes, which typically occur in the gradient zone as discussed in [9].

The dataset obtained by the procedure described above is shown in figure 1. It is seen that the normalised density gradient $(\nabla n_e / n_e) / (\nabla T_e / T_e)$ varies by a factor of four and the normalised particle flux $\Gamma_e T_e / Q$ varies by an order of magnitude. The variation in $\Gamma_e T_e / Q$ is mainly achieved by the inclusion of plasmas with different mixtures of heating powers from purely RF-heating to mixed NBI/RF to purely NBI-heating. The plasmas heated purely by RF, i.e. where NBI heating was absent, or just kept at low power to provide the charge-exchange diagnostics are indicated by open symbols in figure 1. For these plasmas only wall neutrals contribute to the particle flux and on figure 1 therefore these data populate the region with $\Gamma_e T_e / Q < 0.01$. On the other hand we include just one data point with counter-NBI to illustrate very large values of particle flux for these plasmas $\Gamma_e T_e / Q \sim 0.07$ (square symbol in figure 1.).

It is seen from the smaller top panel of figure 1 that parameters such as safety factor and the ratio of electron to ion temperatures are almost constant across the dataset. The ratio of temperature gradients $\nabla T_e / \nabla T_i$ is not shown but is also around unity. The electron temperature-gradient length $\nabla T_e / T_e$

varies by factor of 1.9 in the dataset. The parameter which is considered to be the most significant in controlling the density gradient is the normalised collisionality ν_* [7, 8]. It is seen from the top panel in figure 1 that this key parameter is also restricted to a relatively narrow interval close to the value expected in ITER standard plasma. For $(\nabla n_e/n_e)/(\nabla T_e/T_e) < 0.7$, there is no systematic variation of ν_* in our dataset. For $(\nabla n_e/n_e)/(\nabla T_e/T_e) > 0.7$, the collisionality is on average lower by $\sim 50\%$, but this drop is too small to be responsible for a significant change in density profile. Note that according to the scalings [8] which consider collisionality as the sole parameter governing density peaking, ν_* has to decrease 10 times in order to increase the density gradient by factor of 2. Therefore we conclude that our dataset is restricted enough so that the correlation between normalised particle flux $\Gamma_e T_e/Q$ and density gradient $(\nabla n_e/n_e)/(\nabla T_e/T_e)$ reflects the genuine inter-dependence between these two dimensionless parameters.

The main parameters $y = \Gamma_e T_e/Q$ and $x = (\nabla n_e/n_e)/(\nabla T_e/T_e)$ are displayed on large lower panel of figure 1. It is clearly seen that these two variables are strongly positively correlated: those plasmas with larger normalised particle flux have more peaked density profiles. Fitting a linear model to the data with x as independent variable and y as dependent variable gives $y = A(x-x_0)$ where $A = 0.0982$ and $x_0 = 0.198$. Using x as independent variable and y as dependent variable gives similar result.

The slope in figure 1 can be associated with the ratio of particle and heat diffusivities assuming that the fluxes are related to gradients by offset linear equations and with the convective heat term being ignored: $\Gamma_e = -D_e \nabla n_e + n_e V$, $\Gamma_e T_e/Q \equiv -\chi_{eff}(\nabla T_e + n_i \nabla T_i)$. Here, V is the particle-pinch velocity, n_i is the ion density, ∇T_e is the electron temperature gradient and ∇T_i is the ion temperature gradient. For $n_e \nabla T_e = n_i \nabla T_i$ the normalised flux is $\Gamma_e T_e/Q = D_e/(2\chi_{eff}) \times [(\nabla n_e/n_e)/(\nabla T_e/T_e) - V/D_e \times T_e/\nabla T_e]$. Accepting a rather strong assumption that across the whole dataset $D_e/\chi_{eff} = \text{constant}$ and $V/D_e \times T_e/\nabla T_e = \text{constant}$, the ratio of diffusivities is related to the slope as $D_e/\chi_{eff} = 2A \approx 0.20$. This value is consistent with previous studies in JET [9], and is close to the values found in ASDEX Upgrade ($D_e/\chi_{eff} = 0.15-0.25$) [22], but about 2-3 times lower than inferred in multivariable fits [16]. Experiments with trace tritium showed the tritium diffusivity in the range of $D_T/\chi_{eff} = 0.3-2$, with low values for high density $q_{95} = 3$ plasmas and high values for low density and high q_{95} plasmas [23]. With the same strong assumption as above ($D_e/\chi_{eff} = \text{constant}$, $V/D_e \times T_e/\nabla T_e = \text{constant}$) thesecond fitting term to the data in the figure 1, $x_0 = 0.198$, could be associated with the second term in the analytical expression for the normalised particle flux, $x_0 = V/D_e \times T_e/\nabla T_e$. This would link the normalised pinch velocity to the temperature gradient length as $V/D_e = 0.198 \nabla T_e/T_e$.

It has to be stressed that the dependence between flux $\Gamma_e T_e/Q$ and the gradient $(\nabla n_e/n_e)/(\nabla T_e/T_e)$ is not necessarily expected to be offset-linear. First reason is that convective heat flux cannot be neglected at strong density peaking $\nabla \ln n_e/\nabla \ln T_e \sim 1$ where it can reach 30% of total heat flux. However more significant is the fact that the range of normalised density gradients is so large that one cannot assume that character of the turbulence and hence D_e/χ_{eff} and $V/(D_e \nabla \ln T_e)$ is the same for both large and low values of $(\nabla n_e/n_e)/(\nabla T_e/T_e)$.

Without the guarantee that the dependence between fluxes and gradients is linear the best platform

for comparison between theory and experimental data are simply the absolute values of fluxes at a given gradients. Here the normalisation of particle flux to the heat flux, as presented in figure 1, provides particularly solid platform for comparison of experimental data with theory. Normalisation of particle flux to heat flux removes, to the first order, the large uncertainty associated with amplitude of the turbulence and brings forward the effects of phase shifts between turbulent variables. This fact has been recognised in fluid turbulence where Prandtl and Peclet numbers play a similar role to the ratio D_e/χ_{eff} in a plasma. This is perhaps the reason why the normalised particle flux $\Gamma_e T_e/Q$ provides rather good agreement between experiment and theory, even in its quasi-linear approximation. As a first example, we refer to the result of reference [24] where the quasi-linear calculations for a JET ELMy H-mode plasma, with somewhat higher plasma collisionality than in our case, gives the normalised flux of $\Gamma_e T_e/Q = 0.05$ at the gradient $(\nabla n_e/n_e)/(\nabla T_e/T_e) = 0.05$. These data are taken from figure 2c of ref [24] for density gradient equal to the experimental value, $\nabla n_e/(\nabla n_e)^{exp} = 1.0$, which according to the list of dimensionless parameters given on page 3 of this paper corresponds to a normalised gradient of $\eta_e = (\nabla n_e/n_e)/(\nabla T_e/T_e) = 1.99$. This result is in very good agreement with our data in figure 1. In addition, the figure 2c of the reference [24] shows that the normalised particle flux is indeed correlated with density gradient, but also demonstrates nonlinear character of this dependence. As a second example we compare our data with quasi-linear model developed in [25]. Here the quasi-linear theory is evaluated for normalised density of $(\nabla n_e/n_e)/(\nabla T_e/T_e) = 1/3$. For collisionality similar to our JET data (and to the ITER standard discharge) the quasi-linear model predicts the ratio of effective diffusivities about $D_e/\chi_{eff} = 0.2$. This value is taken from figure 1 of reference [25] for abscissa $[v_{ei}/(c_s/a)]^{0.5} = 0.15$, where v_{ei} is the electron-ion collision frequency and c_s is the sound speed. Such a value is equivalent to the normalised particle flux of $\Gamma_e T_e/Q = (D_e/2\chi_{eff}) [(\nabla n_e/n_e)/(\nabla T_e/T_e)] = 0.033$. This value is again in a good agreement with the JET data in figure 1 at corresponding gradient. These two comparisons may indicate that quasi-linear approximation predicts the correct ratio between particle and heat fluxes while the amplitudes of individual fluxes differ from experimental values.

The offset x_0 determined by data in figure 1 provides a constraint for density profiles in ITER. For standard ITER plasmas neither gas puffing nor pellets are expected to penetrate into the core [26]. The only direct contribution to core particle flux is expected to be due to neutral-beam injection and thus the normalised flux at mid radius is about $\Gamma_{beam} T_e/Q \approx (P_{beam}/P_{loss})(T_e/E_{beam}) \approx 0.003$, where $P_{beam}/P_{loss} = 33MW/130MW$ is the ratio of beam power to total plasma power loss and $T_e/E_{beam} = 12.5keV/1keV$ is the ratio of mid-radius electron temperature to the beam energy expected in ITER [1]. The beam deposition profile is likely to be less peaked than the alpha-particle heating profile and therefore the value of $\Gamma_{beam} T_e/Q$ will be even smaller than estimated above where independence of Γ_{beam}/Q on minor radius is assumed. Such a value of particle flux is much smaller than in most of the JET plasmas and therefore the density profile in ITER can be estimated only by corresponding extrapolation. From figure 1 the normalised density gradient at zero particle flux can be predicted to be approximately in the range of :

$$(\nabla n_e/n_e)/(\nabla T_e/T_e)_{\Gamma=0} \approx 0.15-0.35$$

The main uncertainty in this estimate is due to the error in particle flux as indicated by vertical error bars in figure 1. The lower bound of each error bar is the particle flux due to the source from neutral beams only, $\Gamma_{e, \min} = \Gamma_{e, \text{NBI}}$. The upper bound includes also the source from wall neutrals, $\Gamma_{e, \max} = \Gamma_{e, \text{NBI}} + \Gamma_{e, \text{wall}}$. The error bar is set to $\Gamma_{e, \text{wall}}$ because this quantity is difficult to calculate with sufficient accuracy. The main problem is that our values are calculated by the one-dimensional neutral-particle module in the TRANSP code (FRANTIC [27, 28]), while in reality in diverted plasmas the wall particle source is strongly two dimensional. Another source of uncertainty is the sensitivity of $\Gamma_{e, \text{wall}}$ to the parameters at the very edge which are not measured routinely. For extensive discussion of these problems and a sensitivity study to edge parameters we refer to our previous paper [9]. It can be seen from figure 1 that the prediction of the range of intercepts depends how one extrapolates the envelopes of error bars. A straight line envelope of upper vertical error bars of all points would cross zero flux at practically zero density gradient while a nonlinear envelope of upper error bars would give larger gradient at zero particle flux. This shows how critically the lower limit for predicted peaking depends on the upper error bar of the particle flux, i.e. $\Gamma_{e, \text{wall}}$. The density gradient at zero particle flux can be convincingly determined only by RF-only heated plasmas (and proper evaluation of wall neutrals). As seen from figure 1 such data with $q_{95} \approx 3.0$ and $n_* \approx n_{*, \text{ITER}}$ are rare in JET. There are a few RF-only plasmas with higher safety factor q_{95} than in our selection window and these plasmas show somewhat larger values of $(\nabla n_e/n_e)/(\nabla T_e/T_e)$ than the data in figure 1 at $\Gamma_e T_e/Q < 0.01$. However, before a clear single-parameter q_{95} scan demonstrates the independence of density profiles from safety factor, it could be misleading to base the predictions to ITER standard discharges on these points.

In order to relate the range of normalised density gradients $(\nabla n_e/n_e)/(\nabla T_e/T_e)_{\Gamma=0} \approx 0.15-0.35$ directly to peaking of density profile one would need a prediction of temperature profile in ITER standard plasma, and this is itself a subject of uncertainty of global and pedestal confinement scalings. Assuming that the temperature profile is linear in r/a with $T_e(r/a = 0.35) \approx 17.5 \text{ keV}$ and $T_e(r/a = 0.8) \approx 6 \text{ keV}$ [1] then the relative temperature difference across the zone $0.35 < r/a < 0.8$ is $\Delta T_e/T_e \approx 1$. This would translate to the relative density difference across the same region of $\Delta n_e/n_e \sim 0.15-0.35$, or using a peaking definition from reference [17]: $n_e(r/a = 0.2)/\langle n_e \rangle_{\text{volume}} \sim 1.2-1.4$ (cylindrical approximation and density profile linear in r/a is used). It has to be noted that these predictions assume that the particle source in ITER is similar to the present gas fuelled plasmas in JET. This is however not expected and the dominant fuelling scheme in ITER will be likely an injection of frozen pellets which will repetitively deposit particles in the region $r/a > 0.7$. Because density gradients respond to the imposed particle fluxes the accurate predictions of density profile in ITER would need to take the pellet particle source into account.

CONCLUSIONS

In conclusion, the main result of this work is that a correlation exists between normalised density gradient and normalised particle flux (i.e. particle source) in the JET H-mode data even with collisionality and other key parameters fixed. This study shows that the particle sources do play a role in shaping the density profiles in tokamaks. Therefore the prediction of density profiles for ITER should include also particle flux as one of the extrapolation variables. Ignoring this parameter would significantly overestimate the density peaking in ITER because the scaling would be based on plasmas with much larger normalised particle flux than expected in ITER. Finally, the fact that the density gradients are not canonical in this sense also means that for accurate predictions of the whole density profile in ITER one has to include realistic particle sources, such as shallow pellets.

ACKNOWLEDGEMENTS

We would like to thank Dr H. Weisen for his valuable comments and pointing us to more JET RF-only shots which have been included in our analysis. The authors acknowledge the comments of Drs T. C. Hender, G. P. Maddison, P. Mantica, A. W. Morris and V. Naulin leading to improvements in the manuscript. This work has been conducted under the European Fusion Development Agreement and was funded partly by the United Kingdom Engineering and Physical Sciences Research Council and by EURATOM. The views and opinions expressed herein do not necessarily reflect those of the European Commission.

REFERENCES

- [1]. International Tokamak Experimental Reactor (ITER), *Final Design Report*, 2001 http://www.iter.org/a/index_nav_4.htm
- [2]. Osborne T. H. *et al.*, 2001 *J. Nucl. Mater.* **290-293** 1013
- [3]. Mahdavi M. A. *et al.*, in Fusion Energy 2000 (Proc. 18th Int. Conf. Sorrento, 2000) (Vienna: IAEA) CD-ROM file EXP1/04 and <http://www.iaea.org/programmes/ripc/physics/fec2000/html/node1.htm>
- [4]. Stober J. *et al.*, 2001 *Nucl. Fusion* **41** 1535
- [5]. Valovic M. *et al.*, 2002 *Plasma Phys. Control. Fusion* **44** 1911
- [6]. Hoang G.T. *et al.*, 2004 *Phys. Rev. Lett.* **93** 135003-1
- [7]. Angioni C. *et al.*, 2003 *Phys. Rev. Lett.* **90** 20503-1
- [8]. Weisen H. *et al.*, 2005 *Nucl. Fusion* **45** L1
- [9]. Valovic M., *et al.*, 2004 *Plasma Phys. Control. Fusion* **46** 1877
- [10]. Garzotti L. *et al.*, 2003 *Nucl. Fusion* **43** 1829
- [11]. Isichenko M. B. , Gruzinov A. V. and Diamond P. H., 1995 *Phys. Rev. Lett.* **74** 4436
- [12]. van Milligen *et al.*, 2005 *Plasma Phys. Control. Fusion* **47** B743
- [13]. Garbet X. *et al.*, 2003 *Phys. Rev. Lett.* **91** 035001
- [14]. Garzotti L. *et al.*, 2007 *Nucl. Fusion* **46** 994

- [15]. Zabolotsky A., Weisen H., Karpushov A., TCV Team, JET EFDA contributors, 2006 *Nucl. Fusion* **46** 594
- [16]. Weisen H. *et al.*, 2006 *Plasma Phys. Control. Fusion* **48** A457
- [17]. Angioni C. *et al.*, 2006 "Scaling of density peaking in H-mode plasmas based on a combined database of AUG and JET observations" submitted to *Nucl. Fusion*
- [18]. Baker D. R. *et al.*, 2000 *Nucl. Fusion* **40** 1003
- [19]. Weisen H. *et al.*, 2004 *Plasma Phys. Control. Fusion* **46** 751
- [20]. TRANSP code, http://w3.pppl.gov/tftr/helpdocs/transp/transp_hlp.htm,
- [21]. Goldston R. J. *et al.*, 1981 *J. Comp. Phys.* **43** 61
- [22]. Stober J. *et al.*, 2003 *Nucl. Fusion* **43** 1265–1271
- [23]. Zastrow K.-D. *et al.*, 2004 *Plasma Phys. Control. Fusion* **46** B225
- [24]. Rewoldt, G., Budny R. V., Tang W. M. *et al.*, 2005 *Physics of Plasmas* **12** 042506
- [25]. Angioni C. *et al.*, 2005 *Physics of Plasmas* **12** 112310
- [26]. Polevoi A. R. *et al.*, 2003 *Nucl. Fusion* **43** 1072
- [27]. Tamor, S., Science Applications Inc., Report No. SAI-023-79-1056LJ, 1979 (unpublished)
- [28]. Tunklev M. *et al.*, 1999 *Plasma Phys. Control. Fusion* **41** 985.

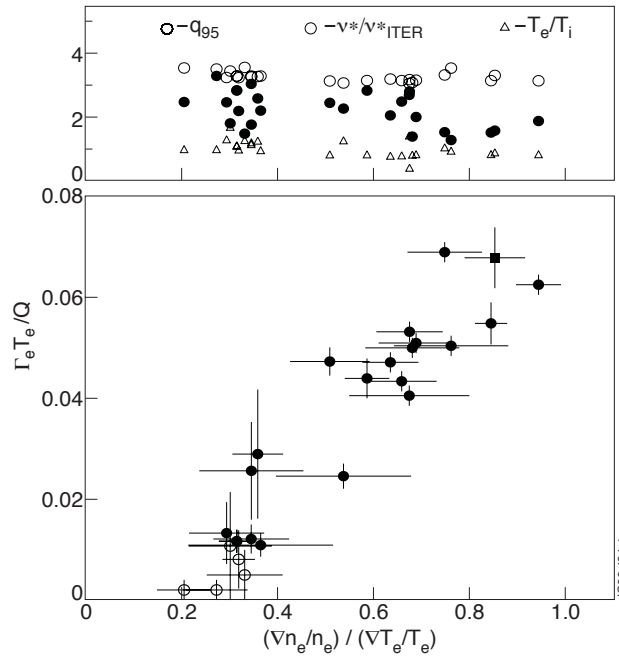


Figure 1: Top panel: The variations of q_{95} (open circles), n^*/n_{*ITER} (full circles) and T_e/T_i (triangles) with density-gradient length normalised to electron temperature gradient length. All quantities (except q_{95}) are taken at $r/a=0.5$. Lower panel: The correlation of normalised particle flux with normalised density-gradient length. The open symbols denote RF-only heated plasmas. The square symbol denotes the only counter-NBI pulse in the dataset. JET Pulse Numbers are: 42981, 43147, 43514, 43522, 50624, 52098, 53171, 53261, 58564, 58894, 59211, 59213, 59214, 59614 (counter-NBI), 59639, 60835, 60854, 61109, 61110, 61164, 61165, 62093, 62094, 62096